Review article

Pushkar Tandon*, Ming-Jun Li, Dana C. Bookbinder, Stephan L. Logunov and Edward J. Fewkes

Nano-engineered optical fibers and applications[1]

Abstract: The paper reviews optical fibers with nano-engineered features and methods to fabricate them. These optical fibers have nano-engineered regions comprising of randomly distributed voids which provide unique properties for designing next generation of fibers. Discussion of impact of void morphology on fiber optical properties is presented, along with the methods to control the void characteristics. Use of nano-engineered fibers for different applications (ultra-low bend loss single mode fiber, quasi-single mode bend loss fiber, endless single-mode fiber, light diffusing fibers) is discussed and the unique optical attributes of the fibers in these applications is highlighted.

Keywords: nano-engineered optical fibers; void morphology; bend-insensitive fibers; endless single-mode fiber; light diffusing fiber.

[1]Invited paper for J. Nanophotonics special issue on "Advances in Fiber Optics Nanotechnology", June 2013.

***Corresponding author: Pushkar Tandon,** Corning Incorporated, Science and Technology, Corning, NY 14831, USA, e-mail: tandonp@corning.com

Ming-Jun Li, Dana C. Bookbinder, Stephan L. Logunov and Edward J. Fewkes: Corning Incorporated, Science and Technology, Corning, NY 14831, USA

Edited by Alan Willner

1 Introduction

Since successful demonstrations of optical fibers with photonic crystal cladding in the late 1990s [1, 2], photonic crystal fibers have attracted significant research interests in the past 15 years. Photonic crystal structures can offer significant advantages over conventional fiber structures in fiber designs, because of their lower effective refractive index and unique dispersion properties. Both the bandgap guiding and average index guiding mechanisms of hole-assisted optical fibers have been extensively studied in the literature. While the periodicity of the holey structure is essential for the bandgap guiding [2], it is not critical for the average index guiding functionality of photonic crystal fibers [3]. In particular, it has been demonstrated that light can be guided in fiber with randomly distributed air holes cladding [4, 5]. Typical processes for making photonic crystal fibers include the stack and draw method [6] or the drilling process. An alternate method of making hole-assisted optical fibers is the use of the nanoStructures™ technology, involving forming of randomly distributed voids in the nano-engineered region of the fiber using traditional optical fiber manufacturing methods such as the Outside Vapor Deposition (OVD), Vapor Axial Deposition (VAD), Modified Chemical Vapor Deposition (MCVD) processes, making the technology ideal for large-scale manufacturing. In this paper, we describe salient features of optical fibers with nano-engineered regions made using the nanoStructures™ technology. Significantly, we discuss the impact of void microstructure (void-fraction, void size and void number density) on the average index guiding behavior of the nano-engineered region at different operating wavelengths and methods to control and obtain the desired microstructure. Different applications are also reviewed which exploit the unique properties of the randomly distributed void filled nano-engineered region. Among the applications include ultra-low bend loss single mode (and quasi-single moded fibers) optical fibers for their use in fiber-to-the-home (FTTH) networks, with the fiber being completely standards compliant and backward compatible [7, 8]. We also disclose use of nano-engineered cladding to design an endless single moded fibers for wide-wavelength window applications. Designs of nano-engineered optical fibers that are 100–200 μm in diameter are also described, which are capable of scattering light through the walls of the fiber across a wide wavelength range and are attractive for illumination applications.

2 Nano-engineered glass features and fabrication

There are different approaches to changing the optical fiber index profiles in designing fibers with desired optical

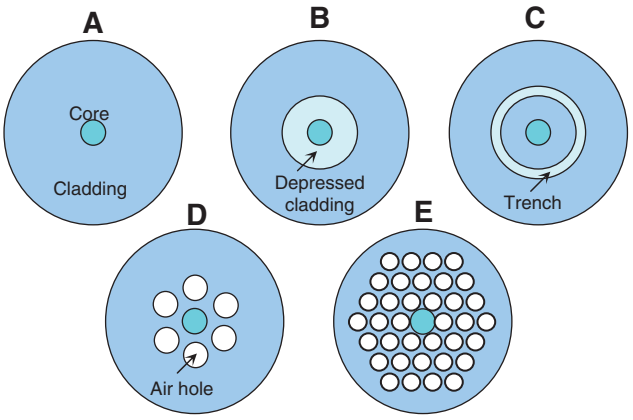

Figure 1 Fiber designs for reducing bending loss: (A) Standard single mode fiber design. (B) Depressed cladding design. (C) Trench fiber design. (D) Hole assisted design. (E) Photonic crystal design.

attributes for telecommunication applications. One conventional design approach involves modifying the index profile for silica based optical fibers using commonly used dopants such as germanium and fluorine. Three conventional designs are shown in Figure 1(A)–(C). Figure 1(A) is an optical fiber design for a standard single mode fiber comprising a core and a clad layer. In Figure 1(B) is shown a fiber with a depressed index inner cladding, while Figure 1(C) shows an optical fiber profile with a depressed index trench in the cladding that is at a radial location offset from the core. In these conventional design fibers, the core region has a refractive index higher than the silica based cladding, with the higher index in the core achieved by doping the region with an up-dopant such as germanium. Similarly, the depressed index regions in Figures 1(B) and 1(C) are obtained by using down-dopants such as fluorine. However, the design window is rather limited with conventional dopants, particularly when the optical fibers are required to be backward compatible and standards compliant.

Second approach for obtaining index lower than that of silica involves use of air holes either in a hole assisted fiber shown in Figure 1(D) or a photonic crystal fiber shown in Figure 1(E). Significant reduction in index can be achieved locally in the hole assisted and photonic crystal fibers, which results in appreciably opening up of the optical design space. However, a typical process for making photonic crystal fibers using the stack and draw process [6] is much more complicated than conventional fiber making processes, thereby making the fibers less attractive for large scale and cost-sensitive applications. An alternate approach for making voids/hole assisted optical fibers is using the nanoStructures™ technology. This technology enables new fiber designs having superior

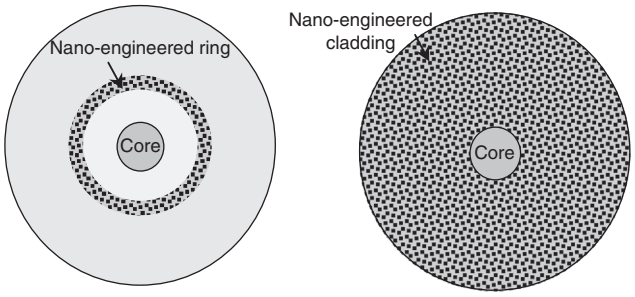

Figure 2 Schematics of two nano-engineered fiber designs.

optical properties, at the same time, maintaining compatibility with large scale manufacturing, legacy fiber plant and existing field installation equipment and procedures.

Figure 2 shows a schematic of the two fiber designs that illustrate use of nano-engineered fibers. The first design consists of a germania-doped core and a nano-engineered ring in the cladding. The ring consists of nanometer-sized gas filled voids that are incorporated in the glass during the fiber processing. These voids are non-periodically distributed in the ring cross-section. The cross-sections of the voids are circular and have diameters ranging from several dozens to several hundreds of nanometers. The void fill fraction can be designed to be between 1 and 10% depending on the ring dimension. The voids are sealed and non-periodically distributed along the fiber length with void lengths ranging from <1 m to several meters. The refractive index profile corresponding to the fiber in Figure 2 in one cross section can be interpreted schematically to be a combination of individual index components of silica and voids, as shown in Figure 3. It is worthwhile to point out that the refractive index profile of the core is axially symmetric, but

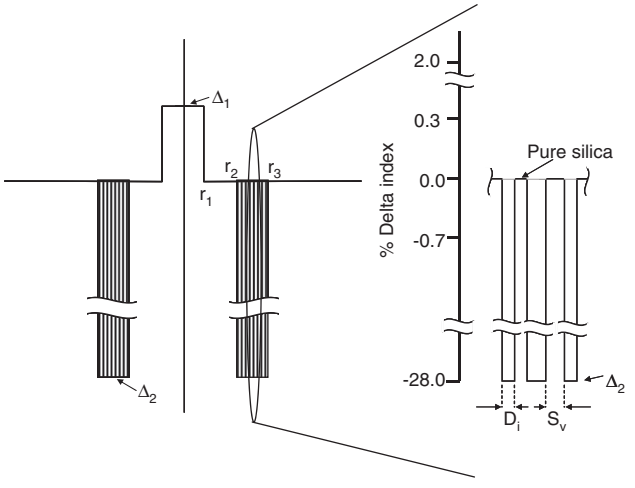

Figure 3 Relative index profile of nano-engineered fiber design.

the refractive index profile of nano-engineered ring is not axially symmetric due to the non-periodic distribution of voids. Because of the non-periodic arrangement of voids, the dimension D_i of each low index region and the space S_v between two adjacent low index regions are not constant. The size characteristics of voids and void fill fraction significantly affect the optical properties of the nano-engineered region, thereby influencing the fiber performance. In the second design shown in Figure 2, the core is comprised of pure silica region with the nano-engineered region making up the cladding layer. The average lowering of the index functionality in the cladding region because of the presence of the voids is able to provide sufficient index differential between the core and the cladding regions and for effective light propagation through the silica core. The void characteristics in the second fiber design are similar to the voids outlined in the first design above.

The optical fiber designs with nano-engineered features offers several advantages compared to other technologies. First, the wavelength dependence of refractive index of glass having nanometer sized features is very different from that of glass with conventional dopants such as GeO_2, F, Al_2O_3, P_2O_5 used in fiber manufacturing. Refractive index profiles of standard optical fibers are typically measured using Refracted Near Field (RNF) method (e.g., High Resolution Optical Fiber Analyzer, Model # NR-9200 HR, EXFO Electro-Optical Engineering). While our attempt to measure the index of the void filled region has not been successful using the RNF method, we have attempted to estimate the effective refractive index of void filled region by considering it to be comprised of periodically distributed voids. To study the sensitivity of the effective index of the void filled glass region to the wavelength and void microstructure characteristics, we have estimated the effective index from the propagation constant of the fundamental space-filling mode β_{FSM} [9]

$$n_{eff} = \frac{\beta_{FSM}}{k}, \quad (1)$$

where $k=2\pi/\lambda$ is the propagation constant of light in the free space. To determine the fundamental space-filling mode, a vectorial finite element method is used to solve Maxwell equations within a unit cell of a periodic structure. Calculations performed on two different periodic structures of triangular lattice and square lattice configurations resulted in similar effective index values, with the results rather insensitive to the lattice structure but strongly dependent on void size and the void fill fraction. In Figure 4 is shown the predicted relative refractive index changes as a function of wavelength for a nano-engineered glass with voids and its comparison with silica doped with fluorine, where the relative refractive index change is defined as $\Delta\%=(n_1^2-n_2^2)x100/2n_1^2$ where n_1 is the refractive index of pure silica, n_2 is the effective index for the nano-engineered glass, or the refractive index of fluorine doped glass. For the illustrative calculations shown in Figure 4, the diameter of the voids in the nano-engineered glass is considered to be 400 nm with a void fill fraction of 2.5%. Correspondingly, the fluorine doped glass shown in Figure 4 has a fluorine doping level of about 2.2% by weight. It is observed that the effective refractive index of nano-engineered glass changes significantly with wavelength, while the corresponding effective refractive index of fluorine doped glass is rather insensitive to the operating wavelength. This characteristic of nano-engineered glass allows us to significantly broaden the design window for making optical fibers with improved optical attributes.

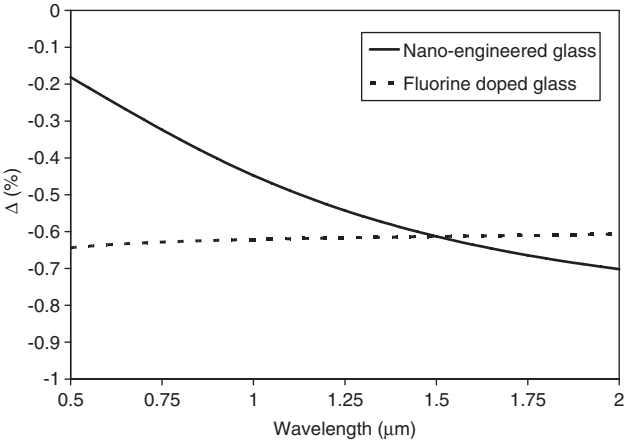

Figure 4 Comparison of relative refractive index changes of nano-engineered and fluorine doped glass.

Nano-engineered fibers can achieve large negative relative refractive index of several percent delta, something that is not possible to obtain with conventional down dopants such as fluorine. Furthermore, the voids in the nano-engineered region can also act as scattering sites, with the scattering magnitude larger at shorter wavelengths. Besides the voids acting as scattering sites, these can also suppress the higher order modes that are bounded by nano-engineered regions.

Methods used for making air-assisted or photonic crystal fiber include stack-and-draw, drilling holes through the preform, etc. However, these methods are cumbersome and not suitable for large scale manufacturing. In contrast, nano-engineered fibers can be made using conventional fiber making processes, making it the technology of choice for high efficeincy manufacturing. During the manufacture of transmission optical fibers

by conventional soot deposition processes such as the outside vapor deposition (OVD) process or the vapor axial deposition (VAD) process, silica and doped silica particles are pyrogenically generated in a flame and deposited as soot. In the case of OVD, silica soot preforms are formed layer-by-layer by deposition of the particles on the outside of a cylindrical target rod by traversing the soot-laden flame along the axis of the cylindrical target. Such porous soot preforms are subsequently treated with a drying agent (e.g., chlorine) to remove water and metal impurities and are then consolidated or sintered into glass blanks at temperatures ranging from 1100–1500°C. Surface energy driven viscous flow sintering is the dominant mechanism of sintering, which results in densification and closing of the pores of the soot, thereby forming a consolidated glass perform. During the final stages of sintering, the gases used in consolidation may become trapped as the open pores are closed. If the solubility and permeability of the trapped gases in the glass are high at the sintering temperature, then the gases are able to migrate through and out of the glass during the consolidation process. Alternatively, gases which are still trapped after the consolidation phase of the fiber manufacturing process may be outgassed by holding the fiber preforms for a period until the gases migrate out through the glass preforms. In consolidation processes which are employed to make conventional transmission optical fiber, the goal is to achieve an optical fiber that is entirely free of voids. Helium is often the gas utilized as the atmosphere during the consolidation of conventional optical fiber preforms because of its high permeability and its ability to easily exit the soot preform and the glass during the consolidation process, so that after consolidating in helium the glass is free of pores or voids. For making of optical fibers with nano-engineered regions, optical fiber preforms are processed under consolidation conditions which are effective to result in a significant volume fraction of gases being trapped in the consolidated glass blank, thereby causing the formation of non-periodically distributed voids in the consolidated glass optical fiber preform. Rather than taking steps to remove these voids, the resultant preform is purposefully used to form an optical fiber with voids therein. In particular, by utilizing relatively low permeability gases (e.g., nitrogen, krypton, sulfur dioxide, etc.) and/or relatively high sintering rates, holes can be trapped in the consolidated glass during the consolidation process. The sintering rate can be increased by increasing the sintering temperature and/or increasing the temperature ramp rate of the soot preform through the sintering zone of the consolidation furnace. Under certain sintering conditions, it is possible to obtain glasses in which the volume fraction of the trapped gases is a significant fraction of the total volume of the preform. The void-containing region can contain over approximately 1,000,000 voids in the cross-sectional slice of the preform wherein the voids can be approximately 1 to 10 microns in average diameter and comprised approximately 1–20 area percent voids. These voids are typically discrete and isolated spheroid shape surrounded by silica, therefore each void is non-continuous in the axial or radial position along the length of the optical preform. When the optical fiber preform is drawn into optical fibers, the voids are stretched along the fiber axial direction, thereby forming the non-continuous voids in the nano-engineered region of the optical fiber [10].

Through experimentation, we have established that the optical properties of the nano-engineered region and that of the fiber comprising such a region are strongly influenced by the void characteristics, such as the void fill fraction, void size and the void number density in the void filled region. While the void fill fraction is more dictated by the preform sintering/consolidation process, the draw conditions and void gas permeability can significantly impact the average void size and void number density in the fiber. During the drawing of the optical fiber preform to an optical fiber, the void fill fraction remains almost constant through the draw process. However, the number of voids (and hence the void number density) decrease significantly in the neck down region of the draw, where the preform is drawn into fiber. For example, a 60 mm diameter preform having 100,000 voids in a cross-sectional ring in the preform can yield 200 voids in the cross-sectional ring for the 125 micron diameter drawn fiber [11]. The reduction in void number is due to "diffusional coalescence" of the voids, i.e., the voids coalesce together to form fewer numbers of voids. In the neck-down or "root" region of the optical fiber preform, the glass temperature increases from above its softening point (approximately 1650°C for silica) to approximately 1900–2100°C (depending on the fiber draw conditions). The fiber then cools back to the softening point, at or after which point the final fiber diameter is reached. The reduction in the number of voids due to diffusional coalescence depends on several parameters including: 1) the diffusivity/permeability of the gas in the voids which migrates through the glass, 2) the temperature-time history the glass experiences in the draw neck-down region, 3) the initial starting distance between the voids, and 4) the resistance to diffusion offered by the glass composition itself. In Figures 5A and B are shown the evolution of number of seeds and void diameter at different axial position in the neck down region for preforms having a low permeability

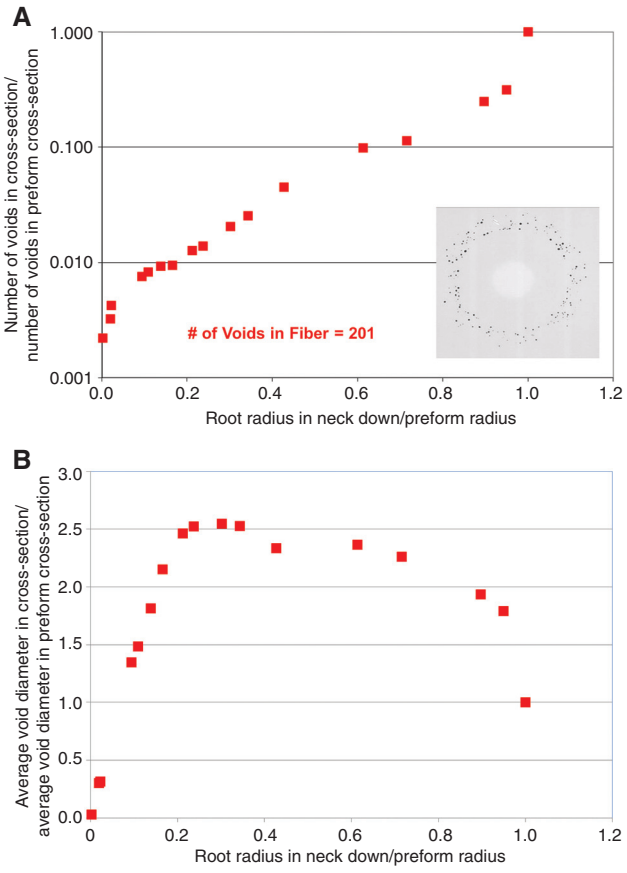

Figure 5 (A) Evolution of number of voids in the neck down region for a preform having voids with a low permeability gas resulting in about 200 voids in the final fiber. (B) Evolution of void diameter in the neck down region for a preform having a low permeability gas in the voids.

gas in the voids. As shown in Figure 5A, the number of voids in the cross-section gradually decreases in the neck down region of the draw due to the "diffusional coalescence" of voids, with the number of voids in the cross-section decreasing by over two orders to magnitude to result in about 200 voids in the fiber cross-section. The size of the voids in the fiber is also influenced by the diffusional coalescence behavior at the draw (Figure 5B). In the upper region of the neck down region of the draw, the void size initially increases due to the void coalescence as well as due to the increase in void gas pressure at the high draw temperatures. The void sizes subsequently decrease in the lower part of the neck down region, where significant draw down of the preform takes place and voids are stretched. In the illustrative example shown in Figure 5B, the average diameter of the voids in the preform increases in the upper part of the neck-down region by a factor of ~2.5 before the voids get stretched in the lower part of the neck down region to result in stretched voids of average diameter of 225 nm in the fiber. Also shown in the inset of Figure 5A is the fiber cross-section with an inner-cladding ring comprising nano-engineered voids that are about 200 in number and having an average diameter of 225 nm. It is clear that to tailor the optical properties of the nano-engineered fibers, it is important to control the void fraction, void size and void number density in the nano-engineered region of the fiber. These void characteristics can be effectively controlled by appropriate choices of void gases, glass composition, consolidation process and draw conditions. For example, by choosing a void gas which had gas permeability in the glass that was significantly lower than the void gas used in examples shown in Figures 5A and B, we were able to appreciably reduce the diffusional coalescence of voids at the draw, resulting in nano-engineered optical fiber with ~450 voids having average void diameter of 125 nm. Similarly, larger number of voids in the fiber is also obtained by using higher draw tension (corresponding to lower peak draw temperature resulting in lower gas permeability) and higher draw speeds (corresponding to reduced time for diffusional coalescence).

3 Nano-engineered fiber designs and application

In this section, we discuss different applications of nano-engineered optical fibers illustrated in Section 2 and fiber designs with desirable void characteristics to obtain fibers with improved optical attributes.

3.1 Ultra-low bending loss single mode fiber

Designing bend insensitive fibers for fiber to the home (FTTH) applications poses significant technical challenges. The first challenge is to reduce the bending loss to meet the requirements of harsh, copper cable-like handling conditions in Multiple Dwelling Units (MDU) applications. This requires a bend-insensitive fiber to have very low (almost zero) bend loss at 1550 nm or shorter wavelength at bend radii typical for FTTH installations. For example in some carrier FTTH deployments bend radii could be as low as 5 mm requiring bend loss to be <0.1 dB/turn [12]. As a reference point, the bend loss of standard single-mode fiber at 1550 nm is typically 20 dB/turn at the same bend radius. This implies a bend loss reduction factor of over 200, which is very difficult to achieve using conventional dopants. The second challenge is to meet the requirements of backward compatibility with the standard single-mode fibers imposed by the telecom industry standards. The bending

and backward compatibility requirements put severe constraints on the fiber design space.

Unique optical characteristics of nano-engineered optical fibers have been exploited to design optical fibers with much better bending performance and with other optical parameters compliant with the standards. The bend performance of a fiber with a low index ring in cladding is determined by the volume of the ring, which is defined as the product of the ring area and the index depression. Increasing the ring volume improves the bend performance. However, the higher ring volume also makes the higher order LP_{11} mode more confined in the core region, which increases the cutoff wavelength. If the ring volume exceeds a certain maximum value, the fiber will exceed the 1260 nm cable cutoff wavelength limit imposed by the G.652 standard. For a fluorine doped ring, the ring volume is constant in the wavelength range between 1200–1600 nm because the index does not change much with wavelength. For a nano-engineered ring design, the ring volume increases with the increase with wavelength. This offers better bend resistance at the more bend sensitive, longer operating wavelengths. At shorter wavelengths the ring volume is reduced, which can keep the cable cutoff wavelength below 1260 nm. As a consequence, the nano-engineered fiber exhibits better bend performance at 1550 nm while retaining complete backwards compatibility with G.652 standard single-mode fibers. To quantify the fiber design advantages, the bending loss of nano-engineered and conventional fluorine trench fibers have been calculated using a bend loss model [8]. Both fibers had the same single mode core design. The inner radius and ring thickness of the nano-engineered ring and the fluorine trench were chosen such that the cutoff, Mode Field Diameter (MFD) and dispersion properties were comparable. To get different cutoff wavelengths and different bending losses, the ring width and void fraction were adjusted for the nano-engineered ring and the width and refractive index are changed for the fluorine trench. For illustrative calculations, a bent fiber is transformed into a straight fiber with an equivalent refractive index distribution as suggested in [13],

$$n_{eq}(x,y)=n(x,y)\exp\left(\frac{x}{R}\right), \tag{3}$$

where R is the bending radius, and the fiber is bent in the x-axis. The numerical modeling is based on a finite element method solving the fully vectorial Maxwell equations used in a previous study [14]. A circular perfectly matching layer (PML) is implemented at the fiber surface to emulate the effect of an infinite domain in the finite element model. With the PML, the propagation constant β of a mode becomes complex with the real part related to the effective index and the imaginary part related to the bending loss. The bending loss of the fiber (α_B) in a particular mode can be calculated from the imaginary part of the propagation constant β so that,

$$\alpha_B=\frac{20}{\ln(10)}\mathrm{Im}(\beta)\approx 8.686\,\mathrm{Im}(\beta). \tag{4}$$

Figure 6 shows the bending loss at 5 mm radius of the two fibers as a function of cable cutoff wavelength. The cable cutoff wavelength is defined as the wavelength at which the loss of the first higher order mode, LP_{11} mode, has a total attenuation of 19.2 dB for a 22 m long fiber with two 80 mm diameter loops as defined in the TIA/EIA FOTP80. The results in Figure 6 show that the nano-engineered fiber has a bending loss of <0.1 dB/turn in the cable cutoff region between 1140 and 1260 nm, which is one tenth of the bend loss of the conventional trench fiber.

Experimental evaluation of the performance of cabled nano-engineered fibers and conventional trench fibers has also been undertaken under extreme deployment conditions, as outlined in [8]. The test conditions are more severe than in typical FTTH deployments and are as follows: 10×90° corner bends+2 bends with 2 kg load+4 wraps at 10 mm diameter+30 staples+10×90° corner bend+1 bend with 14 kg load+6 wraps at 10 mm diameter+50 staples+10 flat staples. For comparison, a conventional trench fiber was tested under the same conditions. Figure 7 plots the attenuation increases at 1550 nm for the two fibers. The conventional trench fiber has a total attenuation increase of almost 2.5 dB. On the other hand, the total attenuation of nano-engineered fiber is about 0.25 dB, which is only one tenth of total attenuation of the conventional trench

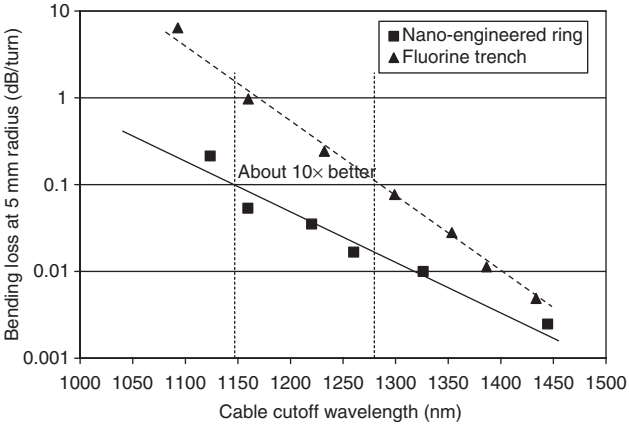

Figure 6 Calculated bending loss at 1550 nm for nano-engineered and conventional trench fibers designs.

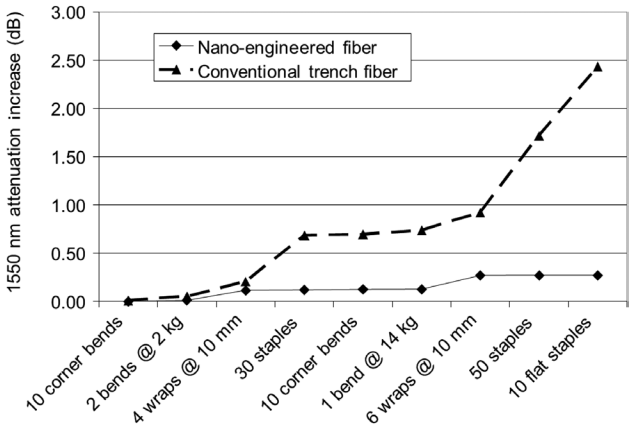

Figure 7 Cabled fiber optical attenuation increases at 1550 nm in FTTH installations described in [8].

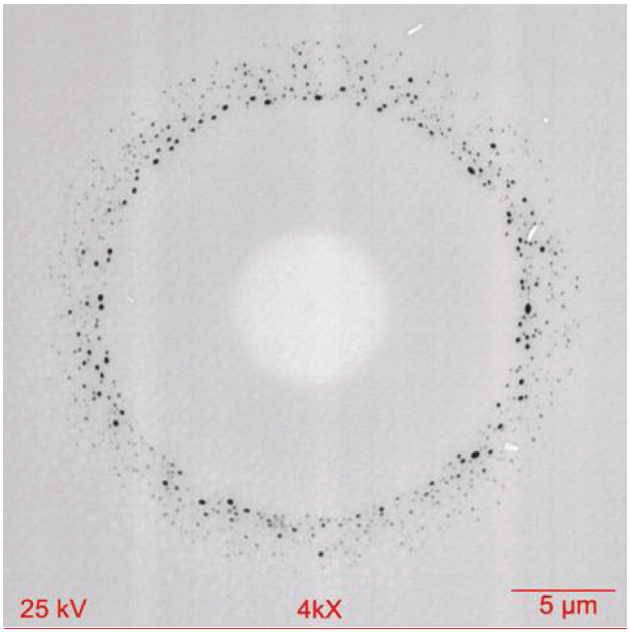

Figure 8 SEM image of a nano-engineered fiber.

fiber. This test demonstrates clearly the advantages of nano-engineered bend-insensitive fiber for FTTH deployments. However, recently advanced fluorine doped trench profiles with additional unique features (not discussed here) have been designed that result in their bend loss performance to be comparable to that of the nano-engineered fibers [15]. Indeed, these unique features can be combined with the nano-engineered fiber technology to yield even lower bend losses and design standards compliant bend insensitive fibers with super-low bend losses.

Optical properties and bending performance of nano-engineered fibers are quite sensitive to the void microstructure. As discussed in Section 2, the number of voids in the ring and the size distribution are strongly influenced by the process conditions used in glass making and subsequent drawing to fiber. It has been established that the fiber bend performance is significantly improved by having the nano-engineered region comprised of an increased number of smaller voids. In Figure 8 is shown an SEM image of a nano-engineered fiber having >400 voids with the mean void diameter of ~130 nm. Increasing the void number density in the ring results in tight packing of the voids, resulting in good bend uniformity not only in the azimuthal direction, but also in the axial direction along the length of the fiber. The radial and axial bend uniformity was determined by measuring bend loss on fiber samples and moving the mandrel location along the length of the fiber in 5 mm increments, and the results are shown in Figure 9. We also report the axial variability measured on a low bend loss fiber using conventional trench design (CTD) and observed that the bend axial and azimuthal uniformity of the nano-engineered (NE) fiber was comparable to the corresponding bend uniformity observed in CTD fibers.

It has also been established that by controlling the void microstructure, the ring volume of the void filled region could be significantly increased compared to the fibers reported in Li et al. [7, 8] and still have cable cutoff wavelength <1260 nm, thereby being fully compliant with standard G.652 single mode fibers. By increasing the void number density (by factor of >2× compared to fibers in Li et al. [7, 8]) and fraction in the fiber, the bend performance of the nano-engineered fibers is improved further. The optical parameters for fibers made with these changes are summarized in Table 1.

Fusion splicing performance has also been evaluated for the nano-engineered fibers, both for homogeneous (NE-NE) and heterogeneous (NE-SMF-28e) splices. For

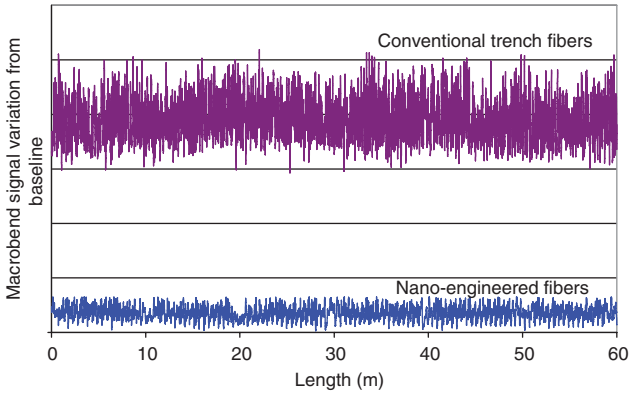

Figure 9 Variation in bend loss along the length of the fiber for conventional trench designs (CTD) and nano-engineered (NE) design.

Table 1 Optical properties of nano-engineered fibers with increased void fraction and void number density.

	Sample A	Sample B	Sample C
Cable cutoff (nm)	1225	1258	1247
MFD at 1310 nm (μm)	8.60	8.48	8.76
MFD at 1550 nm (μm)	9.61	9.56	9.94
Macrobend 1550 nm loss at 5 mm radius (dB/turn)	0.021	0.029	0.012
Zero dispersion wavelength (nm)	1317	1316	1315
Dispersion slope (ps/nm^2/km)	0.089	0.089	0.09
Attenuation at 1310 nm (dB/km)	0.34		
Attenuation at 1550 nm (dB/km)	0.20		

this study, two different splicers were evaluated with active and passive V-groove alignment. For the active alignment splicers, factory preset multimode program was used, while factory pre-set single-mode program was used for the passive alignment splicer. The average splice loss (averaged over 25 splices) was measured to be between 0.05 and 0.08 dB for both heterogeneous and homogeneous splices over the complete wavelength range of 1310 nm–1550 nm on all the splicers (Figure 10).

Quasi single-mode fibers have also been made with thick rings of nano-engineered voids. While these fibers do not meet the cut-off requirement of G.652, they can be used as a single-mode fiber if a restricted launch into the core is used. The advantage of this type of fiber is that the bending loss is even lower. The bending loss of this fiber is <0.01 dB/turn at 5 mm bend radius and <0.001 dB/turn at 10 mm bend radius, which are similar to the bend losses of the hole-assisted bend resistant fibers reported in Refs. [16] and [17]. However, the manufacturing process for making quasi single-mode fibers using nano-engineered voids is much simpler compared to processes used for making hole-assisted fibers.

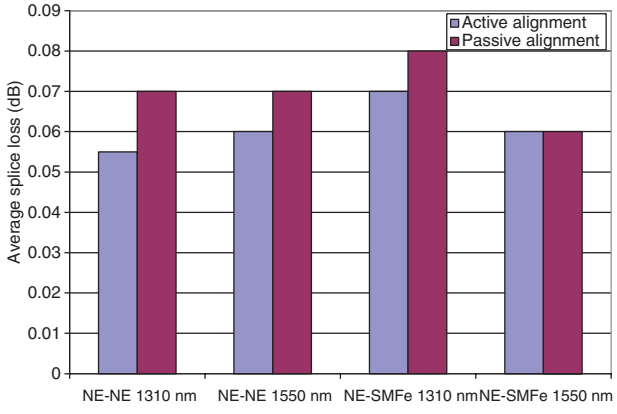

Figure 10 Average splice loss for homogeneous (NE-NE) and heterogeneous (NE-SMFe) splices using splicers with active and passive alignment.

3.2 Endless single moded optical fiber

The second design shown in Figure 2 has a pure silica core and a nano-engineered cladding. This design does not require any conventional dopants in the core and the cladding regions. Both single-mode or multimode fibers can be designed by changing the core size and void fill fraction in the cladding. For single-mode designs, the wavelength dependent effective index property of nano-engineered cladding can be used to design a fiber with very wide single-mode operating window. While the details of the different designs and optical properties are discussed in [18], as an example, Figure 11 shows a measured spectral attenuation of an endless single-moded fiber with a pure silica core and a nano-engineered cladding. The fiber is single moded over the complete measured wavelength range of 600–1700 nm.

3.3 Light diffusing fiber

Optical fibers with nano-engineered features in the fiber core acting as scattering centers provide very efficient

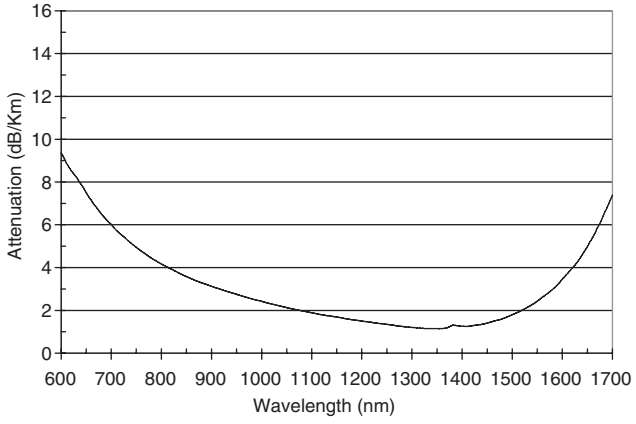

Figure 11 Attenuation spectrum for an endless single-moded fiber with pure silica core and nano-engineered cladding.

scattering of light through the sides of the optical fiber and these light diffusing fibers are important for applications such as specialty lighting, signage and display applications where select amounts of light need to be provided in an efficient manner to the specified areas. Both the small size and the scattering mechanism employed in the fiber afford a very small, flexible illumination source. Nano-engineered light diffusing fibers can also be bundled together to effectively increase the core size to more effectively couple light from LED's and similar light sources. The extraction of light from the fiber is very uniform and may be tuned to scatter more or less light through the sides by controlling the number of scattering sights within the core of the fiber. The emitted light may also be converted to different colors by the use of phosphor coatings.

The light diffusing fiber has a silica core in which a section of the core contains a ring of non-periodically distributed (radially and axially) nano-engineered features acting as scattering sites [19]. The scattering sites have diameters in the ~50–500 nm range and lengths of ~10–1000 mm [19]. Since the scattering centers range in size from 50 to 500 nm, they effectively scatter the propagating light almost independent of the wavelength of the light used. The magnitude of scattered light may be controlled by exploiting its dependence on the size of the scattering centers and their relative area compared to the fiber core. The absorption losses within the fiber are negligible, and the scattering losses can be as high as 5–7 dB/m. The clad of the fiber is either F-doped silica or low index polymer clad, giving NA of the fiber up to 0.53. The bending losses are also small with minimum bending diameters as small as a 5 mm radius.

The large core size and high NA of the fiber allows for low loss coupling of light from inexpensive laser sources, such as visible or near infrared (NIR) laser diodes, with overall efficiencies higher than 85%. Coupling from other types of lasers with reasonable beam quality can also be done with very high efficiency. The relatively low cost of blue diode lasers (405 or 445 nm) creates an economically feasible route to scattering visible light with different colors by placing one or more phosphors in the coating of the fiber. In addition, other scattering materials also can be placed in the coating to provide a fiber with a uniform angular scattering distribution. Several of these fibers were bundled together to couple extended light sources, such as LED or high brightness lamps, into the fiber. Bundles with ~40 light-diffusing fibers have demonstrated coupling efficiency of ~40% to LED sources. The use of nano-engineered light diffusing fibers in illumination applications has been demonstrated in a variety of potential applications and exhibit

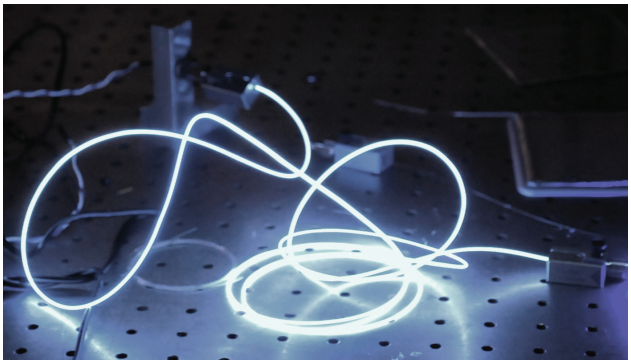

Figure 12 White colors light diffusing fiber with 445 nm laser diode as a source and with "effective length" ~1.5 m. The color conversion of blue light to white is done using Ce-YAG phosphor placed in the coating of the fiber. The diameter of the fiber is 500 μm, glass core diameter 125 micron.

following benefits: The flexibility of thin glass fibers enables the LDF to be deployed in complex configurations and shapes in special lighting applications. Light from the fiber can also be coupled into glass sheets for illumination purposes. The use of yellow phosphor such as Ce-YAG on the surface of the fiber allows for making of bright white color flexible light source. In Figure 12 is shown a nano-engineered light diffusing fiber with the brightness of the fiber exceeding 10,000 lux. This type of fiber, due to its small size, can be coupled to flat glass to make a very low bezel flat illumination fixture similar to back light unit (BLU) used for LCD displays. Figure 13 shows transparent glass plate with LDF coupled to the side of 0.7 mm glass. The glass has a coating on the surface, which scatters light coupled to the wave-guiding

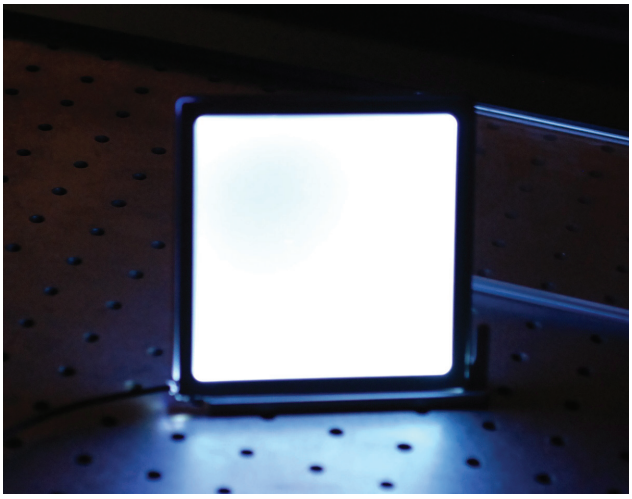

Figure 13 4"x4" glass plate with scattering top layer with LDF coupled to the side of the plate. The 445 nm diode is 1 W, brightness of the plate ~1000 nits.

plate. Furthermore, the light diffusing fibers can be easily connected to low loss delivery fiber, thereby allowing a light source to be remotely placed away from light diffusing portion of the fiber. This helps to deal with heat dissipation and bring additional flexibility to the lighting fixture designs.

4 Conclusions

We have here reviewed optical fibers comprised of regions with nano-engineered voids and discuss the unique optical properties of these fibers. The nanoStructures™ technology described here is compatible with large scale platforms (e.g., OVD, VAD, MCVD, etc.) for making these fibers. It is determined that the optical characteristics of the nano-engineered region is strongly influenced by the void morphology properties of void fraction, void size and void number-density. We disclose the impact of different process parameters on the void morphology and methods to control and obtain desired void characteristics. Different applications that exploit the unique properties of the nano-engineered fibers are discussed and these include ultra-low loss standard's compliant single-mode fiber, quasi-single mode optical fiber, endless single-mode fiber and light diffusing fiber for illumination.

Received July 12, 2013; accepted October 1, 2013; previously published online October 26, 2013

References

[1] Knight JC, Birks TA, St. Russell PJ, Atkin DM. All-silica single-mode optical fiber with photonic crystal cladding. Opt Lett 1996;21:1547–9.
[2] Knight JC, Broeng J, Birks TA, St. Russell PJ. Single mode photonic band gap guidance of light in air. Science 1998;282:1476–8.
[3] Monro TM, Richardson DJ, Broderick NGR, Bennett PJ. Holey optical fibers: an efficient modal model. J Lightwave Technol 1999;17:1093–120.
[4] Monro TM, Bennett PJ, Broderick NGR, Richardson DJ. Holey fibers with random cladding distributions. Opt Lett 2000;25(4):206–8.
[5] Allan D, Borrelli N, Fajardo J, Fiacco R, Hawtof D, West J. Photonic crystal fiber. US6243522, June 5, 2001.
[6] Poli F, Cucinotta A, Selleri S. Photonic crystal fibers: properties and applications, Dordrecht, Netherlands: Springer; 2007.
[7] Li M-J, Tandon P, Bookbinder DC, Bickham SR, McDermott MA, Desorcie RB, Nolan DA, Johnson JJ, Lewis KA, Englebert JJ. Ultra-low bending loss single-mode fiber for FTTH. OFC/NFOEC2008, paper PDP10, San Diego, California, February 24, 2008.
[8] Li M-J, Tandon P, Bookbinder DC, Bickham SR, McDermott MA, Desorcie RB, Nolan DA, Johnson JJ, Lewis KA, Englebert JJ. Ultra-low bending loss single-mode fiber for FTTH. J Lightwave Technol 2009;27(3):376–82.
[9] Birks TA, Knight JC, St. Russell PJ. Endlessly single-mode photonic crystal fiber. Opt Lett 1997;22(13):961–3.
[10] Bookbinder DC, Fiacco RM, Li M-J, Murtagh MJ, Tandon P. Microstructured optical fibers and methods. US 7,450,806, 2008.
[11] Bickham SR, Bookbinder DC, Li M-J, Tandon P. Microstructured transmission optical fiber. US 8,175,437, 2012.
[12] Chen DZ, Belben WR, Gallup JB, Mazzali C, Dainese P, Rhyne T. Requirements for bend insensitive fibers for verizon's FiOS and FTTH Applications. paper NTuC2, OFC/NFOEC2008, San Diego, California, 2008.
[13] Heiblum M, Harris JH. Analysis of curved optical waveguides by conformal transformation. IEEE J Quantum Electron 1975; QE-11:75–83.
[14] Li MJ, Chen X, Nolan DA, Berkey GE, Wang J, Wood WA, Zenteno LA. High bandwidth single polarization fiber with elliptical central air hole. J Lightwave Technol 2005;23:3454–60.
[15] Bookbinder DC, Li M-J, Tandon P. Low bend loss optical fiber. US 8,385,701, 2013.
[16] Nakajima K, Hogari K, Zhou J, Tajima K, Sankawa I. Hole-assisted fiber design for small bending and splice losses. IEEE Photon Technolol Letters 2003;15(12):1737–9.
[17] Bing Y, Ohsono K, Kurosawa Y, Kumagai T, Tachikura M. Low-loss holey fiber. Hitachi Cable Review 2005;24:1–5.
[18] Li M-J, Tandon P, Bookbinder DC, Logunov SL, Kozolov V. Endless single mode optical fibers. Prepared for submission to Nature Photonics, 2013.
[19] Bickham S, Fewkes E, Bookbinder D, Logunov S. Optical fiber illumination systems and methods. US patent application US20110122646A, 2011.